

EVOLUTION OF THERMAL CONDUCTING CLOUDS EMBEDDED IN GALACTIC WINDS

A. Marcolini,¹ D. K. Strickland,² A. D’Ercole³ and T. M. Heckman²

¹*Dipartimento di Astronomia, Università di Bologna, via Ranzani 1, 44127 Bologna, Italy*
andrea.marcolini@bo.astro.it

²*Physics and Astronomy Department, Johns Hopkins University, Homewood Campus, Baltimore, MD 21218, USA*

³*Osservatorio Astronomico di Bologna, via Ranzani 1, 44127 Bologna, Italy*

Abstract We performed high resolution hydrodynamical simulations of dense cool clouds embedded in supernova-driven galactic superwinds. Here we present preliminary results of our reference model in which the effect of heat conduction are taken into account. Significant dynamical differences occur between simulations with and without heat conduction. In absence of heat conduction the cloud fragments in few dynamical timescale. The inclusion of heat conduction has the effect to stabilize the cloud and inhibit the growth of Kelvin-Helmholtz and Rayleigh-Taylor instabilities. Furthermore in the conditions met in our simulations the strong heat flux at the cloud edge generates a converging shock which compresses the cloud. We also calculate the high energy emission (OVI and soft X-ray) of the cloud and OVI absorption line properties and compare the results with observations. Models in which heat conduction is taken into account seem to fit the observations much better. In general only a small fraction (0.1-0.4%) of the wind mechanical energy intersecting the cloud is radiated away. Finally some of our models are able to explain the low metallicity abundance seen in X-ray observation of superwinds.

1. Introduction

Superwinds are multi-phase, loosely-collimated galaxy-sized outflows with measured velocities in excess of several hundred to a thousand kilometers per second, driven from galaxies experiencing intense recent or ongoing star-formation, i.e. starburst galaxies. Superwinds are believed to be driven by the thermal and ram pressure of an initially very hot ($T \sim 10^8$ K), high pressure ($P/k \sim 10^7$ K cm⁻³) and low density wind created from the merged remnants of very large numbers of core-collapse supernovae (SNe). The thermalized SN

and stellar wind ejecta predicted by this model is too hot and too tenuous to be easily observed. However hydrodynamical models of superwinds show that the wind fluid sweeps up and incorporates larger masses of ambient galactic disk and halo interstellar medium (ISM) into the superwind, material which is more easily detected observationally. Recent observations of OVI absorption and emission from $T \sim 10^{5.5}$ K gas in the far Ultraviolet, and thermal emission from $T \sim 10^{6-7}$ K gas in X-ray regime, have shown that the majority of the soft X-ray emission in superwinds is not due to the wind fluid itself, but arises from some form of interaction between the wind gas and denser ambient disk or halo ISM. Here we present preliminary results of high-resolution hydrodynamical simulations of the interaction of a superwind with an embedded cool cloud. In this model we include the effect of thermal conduction, which we show plays an important role in shaping both the dynamics and radiative properties of the resulting wind/cloud interaction. We compare the simulated OVI and soft X-ray properties to the existing observational data.

2. Physical Assumptions and Computational Method

In our models we make the following simplifying assumptions: the clouds are initially spherical, at rest and in pressure equilibrium with the ambient gas; magnetic fields and cloud self-gravity are neglected.

We run several models with different values of the wind temperature T_w ($10^6 - 10^7$ K), wind hydrogen number density $n_{H,w} = n_w = (4.1 \times 10^{-3} - 8.2 \times 10^{-4} \text{ cm}^{-3})$ and wind velocity $v_w = (447 - 2236) \text{ km s}^{-1}$. Here we present results relative to the model with $T_w = 5 \times 10^6$ K, $n_w = 8.2 \times 10^{-4} \text{ cm}^{-3}$, $v_w = 1000 \text{ km s}^{-1}$. The cloud properties are the same in all models: radius $R_c = 15 \text{ pc}$, temperature $T_c = 10^4 \text{ K}$ and density $n_{H,c} = n_c = 0.41 \text{ cm}^{-3}$ (total mass $\sim 206 M_\odot$).

We integrated the hydrodynamical equations with a 2D hydrocode developed by the Bologna group. It is based on an explicit, second order upwind method which makes use of the van Leer interpolation method and of the consistent advection. The method operates on a staggered grid and is implemented with thermal conduction. Following Cowie and McKee (1977) we adopt saturated fluxes to avoid unphysical heat transport in presence of steep temperature gradients. The model presented here is run on a grid with 1200×400 mesh points, with a central uniform region of 1000×300 points and a mesh size $\Delta R = \Delta z = 0.1 \text{ pc}$, while in the outer regions the mesh size increases logarithmically.

Calculations of the OVI and soft X-ray luminosities and 2-dimensional maps of the volume emissivities from these models were performed separately from the simulations themselves. We assumed that the plasma is in collisional ionization equilibrium. The OVI emissivities we use are based on the MEKAL

hot plasma code (e.g. Mewe et al 1985). Note that the luminosity quoted is the sum of the two lines in the $\lambda = 1032 \text{ \AA}$ and 1038 \AA doublet. The soft X-ray luminosities we quote are in the 0.3-2.0 keV energy band, chosen to correspond to the energy band used in the *Chandra* ACIS observations we compare to. The X-ray emissivities used are based on the 1993 update to the Raymond & Smith (1977) hot plasma code. For convenience we calculated all luminosities and volume emissivities assuming Solar abundances (as given in Anders & Grevesse 1989), which is the commonly used standard in X-ray astronomy), although the cloud and wind material may well have different metal abundances.

3. Hydrodynamics

As the wind moves supersonically (Mach number = 3.2) a bow shock forms around the cloud, while a transmitted shock is driven into the cloud. In absence of heat conduction such an interaction leads to a fragmentation of the cloud due to Kelvin-Helmholtz (K-H) and Rayleigh-Taylor (R-T) instabilities (e.g. Klein et al. 1994; Fragile et al 2004) in a typical timescale $\sim (n_c/n_w)^{1/2} R_c/v_w$ ($\sim 3.3 \times 10^5$ yr for this model).

The inclusion of heat conduction has the effect of stabilizing the cloud, as it has the tendency to smooth out the temperature and density gradients such that the K-H instability is noticeably reduced. The heat conduction flux is also responsible for the reduction of the R-T instability.

In fact, in the conditions met in our simulations, the strong heat flux at the cloud edge generates a converging shock which compresses the cloud (Cowie and McKee 1977); the reduction of the cloud size implies a reduction of the momentum transfer from the superwind to the cloud, and thus of the cloud acceleration responsible of the R-T instabilities. As a consequence the cloud remains more compact with bound edges.

The behavior of the cloud is shown in Fig. 1. After 0.15 Myr the cloud is still roughly spherical; however the formation of the converging shock at its edge is clearly visible. At 0.30 Myr the cloud reaches its minimum size and then re-expands mostly downstream where it is not contrasted by the effect of the ram pressure of the incoming superwind. The shrinking of the cloud leads to a reduction the evaporating rate \dot{M} that varies in pace with the radius. After 1 Myr the cloud retains half of its initial mass while the rest has evaporated and mixed with the superwind material.

In general we found that due to dynamical effect, the lifetime of our evaporating clouds is 2-3 times longer than that provided by the analytical solution of a steady evaporation cloud (see Cowie & McKee 1977). It turns out that the cloud can survive from 1-13 Myr depending on the parameters of the wind.

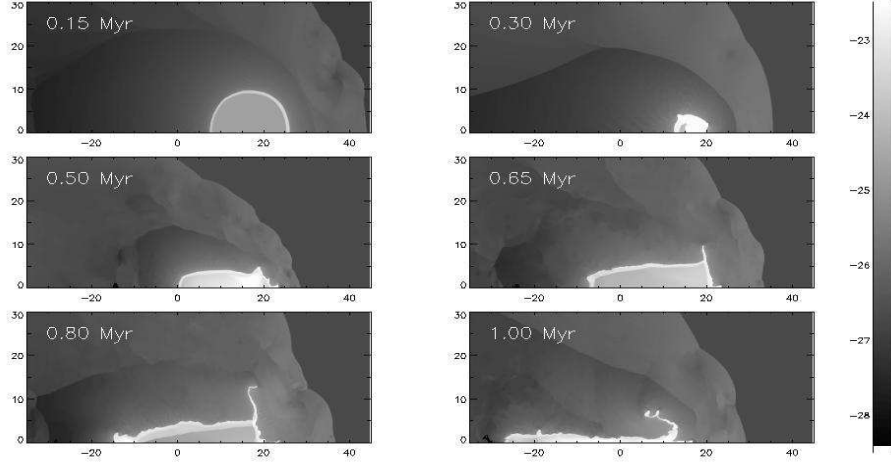


Figure 1. Density distribution at different times of the cold cloud interacting with the hot tenuous superwind including the effects of heat conduction. The logarithm of the mass density (in units of g cm^{-3}) is shown. The distances are given in pc. At the beginning of the simulation the cloud centre is at $z = 20$ pc.

4. OVI and X-ray Emission

Figure 2 shows the OVI and the X-ray maps of the model presented here. As a gas element evaporates from the cloud, it quickly goes through a large interval of temperatures, ranging from $T \sim 3 \times 10^5$ K where the OVI emission peaks, up to X-ray temperatures (several 10^6 K). Thus significant OVI and X-ray emissions originate close to the cloud surface, and are spatially connected. For this reason their time evolution is connected to the cloud dynamics, in particular to the variation of the cloud density at R_c and to the evolution of the cloud size.

The OVI luminosity L_{OVI} oscillates in time between 6×10^{32} and 10^{34} erg s^{-1} with a period of 0.7 Myr (see Fig. 3). The X-ray luminosity L_X oscillates with the same period, but to a lesser extent between 1.5×10^{33} and 6×10^{33} erg s^{-1} . This lower amplitude is due to the fact that the soft X-ray flux originates not only close to the cloud surface, but also behind the bow shock; this second component is quite steady and reduces the overall X-ray variability. We point out that the OVI and X-ray luminosities have a maximum at the leading edge of the cloud close to the symmetry axis, where the density of the evaporating gas is maximum. This is due in part to the larger temperature of the shocked superwind, and partially to the compression given by the ram pressure. From Fig. 3 is clear that in the model in which the effect of heat

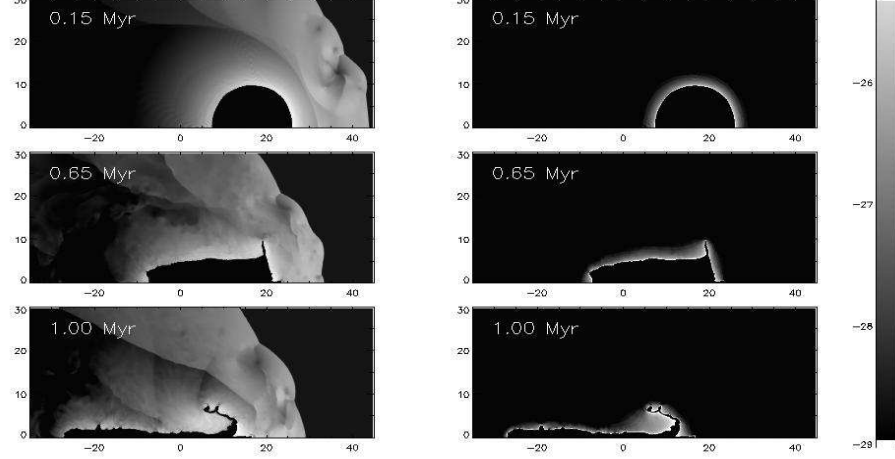


Figure 2. X-ray (left panels) and OVI (right panels) volume emissivity at 3 different times. The logarithm of the soft X-ray (0.3 – 2.0 keV energy band) and OVI volume emissivity (in units of $\text{erg s}^{-1} \text{cm}^{-3}$) is shown.

conduction is neglected, both L_X and L_{OVI} are increasing with time according to the fragmentation of the cloud.

In general only a small fraction (0.1 – 0.4%) of the mechanical energy of the wind that collides with the cloud is radiated away from the cloud itself at FUV and X-ray wavelengths.

Being the physical size of the observational *FUSE* 30" aperture dependent on the distance to the observed galaxies (equivalent to ~ 530 pc for M82, and for ~ 2.5 kpc for NGC 3079), and that we do not know how many clouds actually lie within these regions, our quantitative comparison to the observational data will concentrate on the ratio of OVI to soft X-ray emission, rather than the absolute emitted luminosities. Actually in our model with conduction the ratio L_{OVI}/L_X assumes the values ≤ 1.0 that are observed in NGC 4631 (Otte et al. 2003) and M82 (Hoopes et al. 2003) for a considerable fraction of the time simulation. We stress that the analogous model without thermal conduction gives a ratio L_{OVI}/L_X much higher, largely out of the observed range.

In addition to calculating the X-ray and OVI emission we also consider absorption line properties, specifically column densities of the OVI ions probed in *FUSE* observations of starbursts (see e.g. Heckman et al. 2001, 2002). The mean value of $\log(N_{\text{OVI}})$ through the center of the cloud averaged over a radius of $R_{\text{SOR}} = 5$ pc is ~ 13.19 for the model without heat conduction and ~ 13.43 for the model with heat conduction.

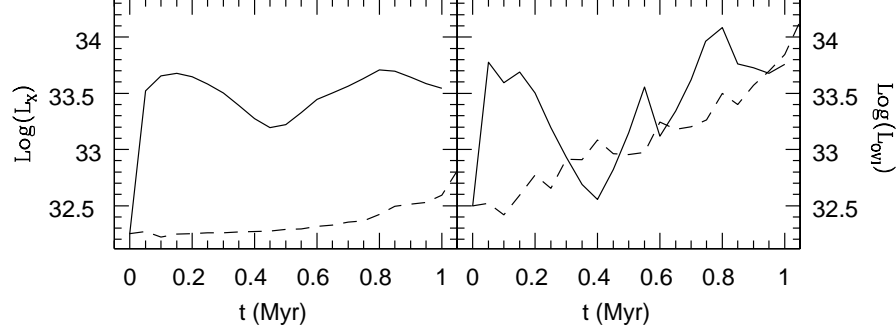


Figure 3. Time evolution of the logarithm of X-ray (left panel) and OV1 (right panel) luminosities for the model with (solid line) and without (dashed line) heat conduction.

5. Chemical Abundance of the X-ray Gas

It is known that the abundance of the X-ray emitting gas in starburst galaxies is rather puzzling. Although the superwind gas is supposed to be composed mainly by SN ejecta, its metal abundance derived from its X-ray emission is consistent with Solar abundance of the α -elements (Strickland et al. 2004a). In our model the emitting gas is composed by a mixture of evaporating cloud gas with metallicity Z_c and enriched superwind material with metallicity Z_w . Thus the observed metallicity is given by $Z_X = Z_c + A(Z_w - Z_c)$, where $A = n_w/(n_c + n_w)$ is weighted by the X-ray emission. Z_X may be quite low for low values of A ; this is actually the case for this model where A varies within the range 0.1-0.4 (i.e. the observed abundance will be $Z_X \sim Z_c$, which should be \sim Solar). Much lower values of A may be obtained varying some parameters: for instance, for $v_w = 2236 \text{ km s}^{-1}$ A can be as low as 0.02.

References

- Anders E., Grevesse N., 1989, *Geochim. Cosmochim. Acta*, 53, 197
Cowie L., McKee C., 1977, *Apj*, 211, 135
Klein R., McKee C., Colella P., 1994, *ApJ*, 420, 213
Fragile C., Murray S., Anninos P., van Breugel W., 2004, *ApJ*, 604, 74
Heckman T., Norman C., Strickland D., Sembach K., 2002, *ApJ*, 577, 691
Heckman T., Sembach K., Meurer G., Strickland D., Mertin C., Calzetti D., Leitherer C., 2001, *ApJ*, 554, 1021
Hoopes C., Heckman T., Strickland D., Howk J., 2003, *ApJ*, 596, L175
Mewe R., Gronenschild E., van den Oord G., 1985, *A&AS*, 62, 197
Otte B., Murphy E., Howk J., Wang Q., Oegerle W., Sembach K., 2003, *ApJ*, 591, 821
Raymond J., Smith B., 1977, *ApJS*, 35, 419
Strickland D., Heckman T., Colbert E., Hoopes C., Weaver K., 2004, *ApJS*, 151, 193